

H-induced subcritical crack propagation and interaction phenomena in (001) Si using He-cracks templates

S. Reboh, J. F. Barbot, M. F. Beaufort, and P. F. P. Fichtner

Citation: [Applied Physics Letters](#) **96**, 031907 (2010); doi: 10.1063/1.3290249

View online: <http://dx.doi.org/10.1063/1.3290249>

View Table of Contents: <http://scitation.aip.org/content/aip/journal/apl/96/3?ver=pdfcov>

Published by the [AIP Publishing](#)

Articles you may be interested in

[Phase-field modeling of diffusion-induced crack propagations in electrochemical systems](#)

Appl. Phys. Lett. **105**, 163903 (2014); 10.1063/1.4900426

[Nanoscale organization by elastic interactions between H and He platelets in Si](#)

J. Appl. Phys. **114**, 073517 (2013); 10.1063/1.4818812

[Localized exfoliation versus delamination in H and He coimplanted \(001\) Si](#)

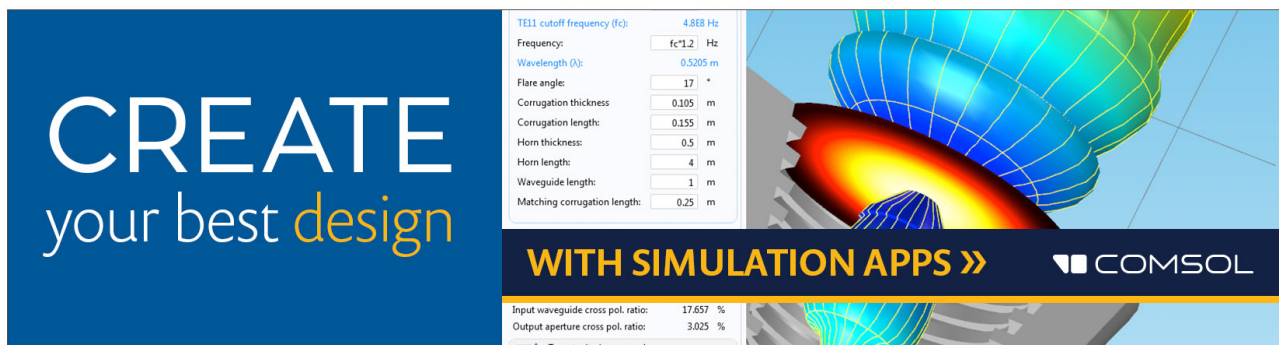
J. Appl. Phys. **105**, 093528 (2009); 10.1063/1.3116738

[H-induced platelet and crack formation in hydrogenated epitaxial Si/Si 0.98 B 0.02/Si structures](#)

Appl. Phys. Lett. **88**, 021901 (2006); 10.1063/1.2163992

[Evolution of hydrogen and helium co-implanted single-crystal silicon during annealing](#)

J. Appl. Phys. **90**, 3780 (2001); 10.1063/1.1389478

An advertisement for COMSOL software. On the left, a blue box contains the text 'CREATE your best design' in white and yellow. In the center, a white panel lists various simulation parameters for a TE11 cutoff frequency, such as Frequency (4.868 Hz), Wavelength (0.5205 m), and Corrugation thickness (0.105 m). On the right, a 3D simulation image shows a horn-shaped structure with a color gradient from blue to red, representing a field distribution. At the bottom, a dark blue bar features the text 'WITH SIMULATION APPS »' and the COMSOL logo. Below this bar, a small white box shows 'Input waveguide cross pol. ratio: 17.657 %' and 'Output aperture cross pol. ratio: 3.025 %', with a checked box for 'Target criterion: passed'.

H-induced subcritical crack propagation and interaction phenomena in (001) Si using He-cracks templates

S. Reboh,^{1,a)} J. F. Barbot,² M. F. Beaufort,² and P. F. P. Fichtner³

¹Groupe nMat, CEMES-CNRS, 29 rue J. Marvig, 31055 Toulouse, France

²PHYMAT-CNRS, Université de Poitiers, SP2MI, BP 30179, 86962 Futuroscope, France

³Escola de Engenharia, Universidade Federal do Rio Grande do Sul, Porto Alegre 91501-970, Brazil

(Received 23 November 2009; accepted 16 December 2009; published online 21 January 2010)

H and He ion implantations allow the formation of nanocracks within controlled subsurface depths in semiconducting materials. Upon annealing, crack propagation and coalescence provides a way of cutting monocrystalline thin films. Here, the mechanisms of coalescence by crack-tip interactions are depicted in (001) Si wafers. Starting from overpressurized He-cracks, subcritical propagation was activated by diffusional H. Nanocrack interaction can occur by elastic forces, causing tip folding, or by plastic deformation forming extended defects. These observations are discussed and modeled using elasticity and fracture mechanics. The model suggests that kinetic effects in the cutting process depend on the crack interplanar separations. © 2010 American Institute of Physics. [doi:10.1063/1.3290249]

Hydrogen induced cracking in semiconducting materials has been extensively studied in correlation with thin layer transfer techniques.¹⁻⁸ Particularly, the formation of cracks lying parallel to the surface and confined to a narrow region within the substrate has been investigated by H (Refs. 1-5) and H+He ion implantation^{6,7} or by plasma hydrogenation methods.⁸ Upon annealing or continuous hydrogenation, crack propagation and coalescence leads to a continuous fracture along the substrate, resulting in the separation of the material overlayer. In combination with wafer bonding techniques, this layer separation process enables the fabrication of high quality silicon-on-insulator (SOI) substrates and, moreover, revealed a versatile route for incommensurable lattice materials integration for advanced microelectronics.³

The lattice damage and compressive in-plane stress produced by the implantation process creates the appropriate conditions to locally trap the H atoms, as well as to induce cracks formation parallel to the surface.⁵ In the case of plasma based techniques, H trapping sites as buried strained layers must be previously introduced in order to define the cracking layer.⁸ The basic aim of such processes is to create conditions for crack formation and propagation parallel to the surface. In this scenario, single crystalline silicon is regarded as a model case material for the study of the physical-underlying mechanisms which could be considered in three major levels as follows: (i) formation of nanocracks, (ii) activation of crack propagation, and (iii) interaction between crack tips leading to cracks coalescence. The first two items have been quite extensively investigated.¹⁻⁸

In the present letter we focus on the study of nanocracks interaction and coalescence processes in nanometer size scale. The experiments have been designed to allow controlled crack propagation, as a result from the incorporation of H atoms into pressurized He-filled cracks⁹⁻¹¹ previously introduced. Transmission electron microscopy (TEM) investigations show that the interaction of cracks can be plastic or elastic. These observations are discussed and modeled in terms of elasticity and fracture mechanics.

The experiments were performed using p-type Czochralski grown (001) Si wafers with a resistivity of 1-25 Ω cm. Wafer pieces were implanted at room temperature with He⁺ ions accelerated at 45 keV to the fluence $\Phi = 1 \times 10^{16}$ cm⁻², and then annealed at 350 °C during 900 or 1800 s. This procedure leads to the formation of overpressurized He-cracks located ≈ 400 nm underneath the surface.¹¹ Some of the He implanted/annealed samples were additionally implanted at 200 °C with 30 keV H₂⁺ ions to the fluence $\Phi = 0.5 \times 10^{16}$ cm⁻². The predicted mean depth range of the H⁺ implantation is ≈ 200 nm.¹² The He/H co-implanted samples were finally subjected to a thermal treatment at 300 °C for 900 s. Microstructure characterization was performed in a JEM 2010 TEM operating at 200 kV.

Figure 1 summarizes the microstructure evolution during the different steps of the process. Figure 1(a) shows a cross sectional TEM image from a sample implanted only with He and annealed at 350 °C for 900 s. It presents two edge-on oriented He-cracks located close to 400 nm depth. The thin central white feature corresponds to the cavity region. The surrounding fringes result from a strain-related contrast induced by the high gas pressure inside the cavities.⁹⁻¹¹ The separation distance between these He-cracks typically exceeds their mean diameter of ≈ 150 nm, resulting in a discrete array of structures preferentially oriented parallel to the surface. Control samples, annealed at 350 °C for 1800 s, show the same microstructure features suggesting that the He-cracks are quite stable with respect to $T \leq 350$ °C. Figure 1(b) provides a general view of the developed microstructure for samples additionally submitted to the H-implantation and annealing step. Nanosized H-platelets are observed at ≈ 200 nm depth. At the depth region originally containing the He-cracks it is now observed a chain of long and flat cracks. This indicates that a crack propagation process driven by a diffusional supply of H atoms took place. Distinct crack interaction effects were identified by the observation of the crack tips structure. These interactions can be of plastic-type, as observed by the formation of dislocations and nanotwin structures connecting the crack tips [Fig. 2(a)], or of elastic-type by stress field interactions resulting in deviations of crack-tip propagation [Fig. 2(b)]. In this last case, the ap-

^{a)}Author to whom correspondence should be addressed. Electronic mail: shay.reboh@ceмес.fr.

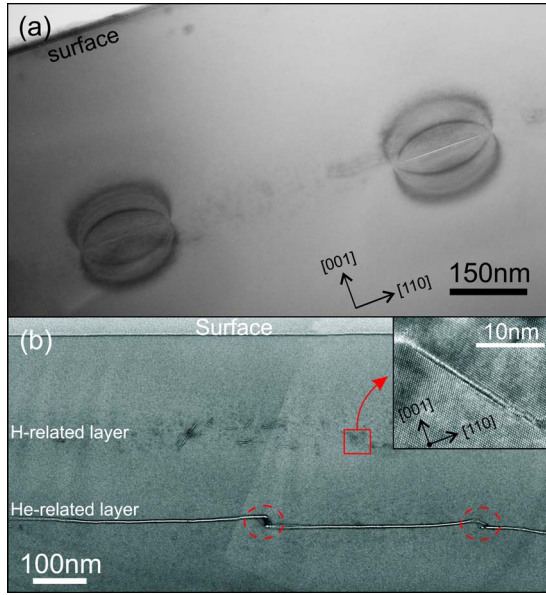


FIG. 1. (Color online) (a) Two edge-on overpressurized He-cracks are seen in a cross-sectional bright-field TEM image (dynamical diffraction condition, overfocus, $g=004$) of He-implanted Si at RT (45 keV, 1×10^{16} cm $^{-2}$) and annealed at 350 °C for 900 s. (b) Bright-field TEM image showing the an overview of the microstructure after H $_2^+$ implantation at 200 °C (30 keV, 0.5×10^{16} cm $^{-2}$) and annealing (300 °C for 900 s). The inset shows in detail one platelet formed in the stopping range of H ions and the dashed circles highlight the regions of cracks tip interaction.

proaching cracks merge by redirecting the propagation direction against each other.

According to elasticity and linear fracture mechanics concepts, an overpressurized He-crack can be defined as a Griffith crack structure holding an internal pressure comprised between its thermodynamic equilibrium pressure with the medium (p_{eq}) (Ref. 13) and the maximum pressure of crack stability (p_{max}).¹⁴ Above p_{max} spontaneous unstable crack propagation occurs.⁷ This process develops when the

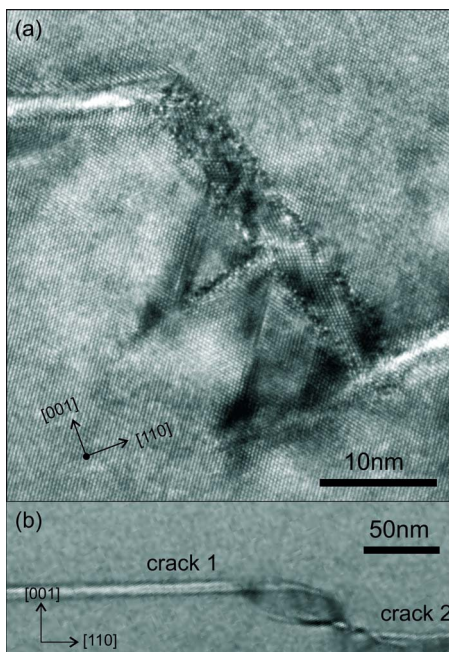


FIG. 2. (Color online) Cross-sectional bright-field TEM image of the different interactions of crack tips (a) plastic-type interaction resulting in the formation of structural defects. (b) elastic-type interaction showing the deviation of the crack propagation resulting in coalescence.

stress intensity factor at the crack-tip, K_I , overcomes the fracture toughness K_{IC} of the material.¹⁵ Hence, an overpressurized state of the He-cracks can be defined for pressures p_{op} in the range

$$p_{eq} = \sqrt{\frac{2\pi\mu\gamma}{(1-\nu)d}} \leq p_{op} \leq p_{max} = K_{IC} \sqrt{\frac{2}{\pi d}}. \quad (1)$$

In Eq. (1) μ is the shear modulus of the medium, ν is the Poisson's ratio, γ is the surface energy and d is the crack diameter (for a Si matrix, $\mu=68$ GPa, $\nu=0.22$, $\gamma=1.38$ J/m 2 and $K_{IC}=1.19$ MPa m $^{1/2}$).⁷ Since spontaneous propagation did not take place upon annealing up to 300 °C, the internal pressure of the He-cracks can be considered to be lower than p_{max} , estimated to be ≈ 2.5 GPa for a He-crack of $d \approx 150$ nm. As a consequence, the relation $K_I < K_{IC}$ hold all along the experiment, implying that the He-crack propagation, observed for samples additionally implanted with H, take place under subcritical conditions. This propagation phenomenon is particularly frequent in cases where the effect of stress is combined with chemically active species as H operating at the crack-tip,¹⁶ and renders a scenario that applies well to the present situation. Throughout the experiments, H atoms could migrate toward the He-cracks, either during the implantation at $T_i=200$ °C or during the post implantation thermal treatments.

When the distance between two crack tips is sufficiently small (below 50 nm), complex interaction phenomena occurs. Figure 2(a) shows that plastic interactions between the crack tips block their growth by the formation of nanotwins. This situation can be qualitatively understood in terms of the shear stress in the lattice region between two parallel noncoplanar approaching cracks. The stress increases as the crack tips approaches and eventually overcome the critical stress for twinning resulting in cooperative strain relief for both cracks. However, when the stress between pairs of parallel crack-tip does not satisfy the stress intensity conditions for plastic deformation, the cracks continue to propagate. These pairs start to interact elastically, leading to a deviation of their propagation direction. This behavior can be predicted in terms of the modification of the stress intensity factor components due to the elastic forces introduced by the approaching second crack. In this context, following the derivations from Gross and Seelig,¹⁵ the modification of the stress intensity factor K_I from an undisturbed crack can be represented by a factor K_I^i , which also affects the driving force controlling the propagation kinetics. Similarly, a factor K_{II}^i represents the antisymmetric component introduced by the interaction, which determines the deviation of the propagation direction. Under near equilibrium conditions [i.e., $K_I \approx \pi \sqrt{\frac{\mu\gamma}{(1-\nu)}}$, see Eq. (1)], these effective interaction factors can be expressed as

$$K_I^i \approx (\pi\beta) \left[1 + \frac{1}{8}(\alpha)^2(2 \cos 2\theta - \cos 4\theta) \right] \quad (2)$$

and

$$K_{II}^i \approx \frac{\pi}{8} \beta \alpha^2 (-\sin 2\theta + \sin 4\theta), \quad (3)$$

where the quantity $\beta = \sqrt{\frac{2\mu}{1-\nu}}$ refers to the mechanical properties of the material, $\alpha = d/L$ defines an adimensional interaction distance and θ is the interaction angle between the two

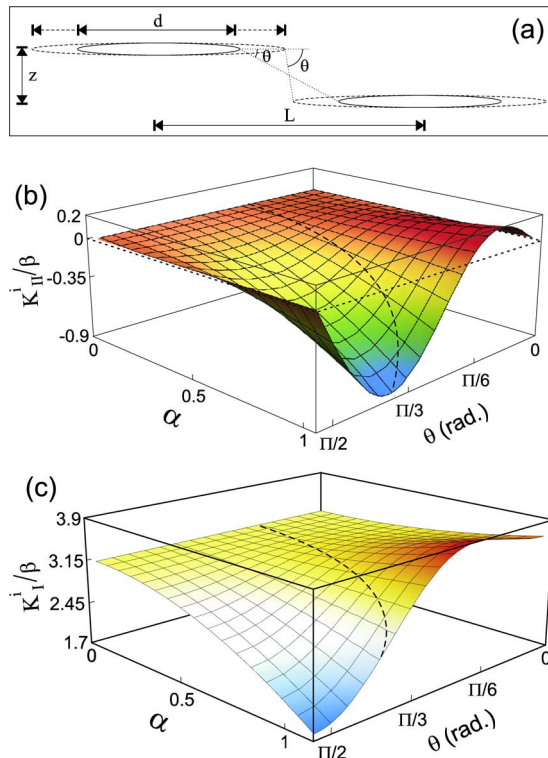


FIG. 3. (Color online) (a) depicts the interaction parameters from Eqs. (2) and (3), d is the crack diameter, L their midpoints distance, θ the interaction angle and Z the depth separation distance. (b) and (c) are the reduced stress intensity factor K_{II}^1/β and K_I^1/β as function of α and θ , respectively.

tips, as defined in Fig. 3(a). The domains of the reduced factors K_I^1/β and K_{II}^1/β as a function of α and θ are graphically presented in Figs. 3(b) and 3(c), respectively. A positive K_{II}^1/β value means a repulsive interaction, resulting in the tendency of crack-tip deviation toward opposite directions. Reversely, negative K_{II}^1/β values mean attractive interaction, causing their redirection toward each other.

For the case of parallel coplanar cracks (i.e., $Z=0$), K_{II}^1/β is null for any value of α , meaning that there is no deviation of the propagation direction. At the same time, K_I^1/β increases with α , suggesting an enhancement of the propagation kinetics as the interacting distance decreases. For noncoplanar cracks (i.e., $Z>0$) the angle θ increases with α . For a sufficient large separation (i.e., small α) K_{II}^1/β values are negligible, therefore the cracks follow an undisturbed straight propagation. As the interaction distance decreases, α and θ increase and therefore K_{II}^1/β becomes negative, setting an attractive elastic force that bends the crack propagation direction toward the counterpart crack, as experimentally observed. Along this interaction path, K_I^1/β value reduces suggesting a reduction in the cracks propagation kinetics. The dotted lines in Figs. 3(b) and 3(c) propose an interaction route for the above situation. Furthermore, for a given α , there is an optimal value of Z for maximum attractive interaction given by $Z=(L-d)tg\theta$ with $\theta\approx\pi/3$. Considering a crack diameter of 500 nm and a distance of 20 nm between the crack tips (i.e., $L=520$ nm) as shown in Figs. 1(b) and 2(b), an optimal value $Z\approx 35$ nm is obtained. This is indeed in good agreement with the experimental situation, and suggests that the present observations were only

possible because of the optimized initial conditions of the He-crack system.

Hence, in order to optimize layer separation processes induced by crack coalescence, the formation of coplanar cracks system with $Z=0$ would provide ideal conditions, not only to reduce the total amount of required H but also to enhance the fracture kinetics. Due to the depth distribution of the implantation damage and the statistical nature of the nucleation process for He or H induced crack structures, the $Z=0$ ideal condition may not occur for initially homogeneous substrates. However, this limitation can be over passed by introducing preferential heterogeneous nucleation sites for cracks, as recently demonstrated for the cases of strained interfaces.⁹

In summary, a diluted system of He-cracks formed by He^+ ion implantation into (001) Si substrates is used as model case structures to study the subcritical propagation of cracks. Three main points were discussed using elasticity and fracture mechanics concepts as follows: (i) the formation of overpressurized He-cracks are expressed in terms of their equilibrium and limit pressures; (ii) the effects of the diffusional supply of H atoms for crack propagation; and (iii) the nanoscale cracks interaction mechanisms are depicted in terms of plastic or elastic interactions. Plastic interactions result in the formation of dislocations and twinlike extended defects due to a high shear stress between approaching parallel crack tips. Elastic interactions cause their deviation from the original propagation direction, resulting into an interlacement of crack tips, as predicted by model calculations.

The authors acknowledge the support from PETROBRAS S. A., CNPq, and CAPES.

- ¹M. Bruel, *Mater. Res. Innovations* **3**, 9 (1999).
- ²M. K. Weldon, V. E. Marsico, Y. J. Chabal, A. Agarwal, D. J. Eaglesham, J. Sapjeta, W. L. Brown, D. C. Jacobson, Y. Caudano, S. B. Christman, and E. E. Chaban, *J. Vac. Sci. Technol. B* **15**, 1065 (1997).
- ³B. Aspar, H. Moriceau, E. Jalaguier, C. Lagaha, A. Soubie, B. Biasse, A. M. Papon, A. Claverie, J. Grisolia, G. Benassayag, F. Letertre, O. Rayssac, T. Barge, C. Maleville, and B. Ghyselen, *J. Electron. Mater.* **30**, 834 (2001).
- ⁴S. Personnic, K. K. Bourdelle, F. Letertre, A. Tauzin, N. Cherkashin, A. Claverie, R. Fortunier, and H. Klocker, *J. Appl. Phys.* **103**, 023508 (2008).
- ⁵M. Nastasi, T. Höchbauer, J. K. Lee, A. Misra, J. P. Hirth, M. Ridgway, and T. Lafford, *Appl. Phys. Lett.* **86**, 154102 (2005).
- ⁶A. Agarwal, T. E. Haynes, V. C. Venezia, O. W. Holland, and D. J. Eaglesham, *Appl. Phys. Lett.* **72**, 1086 (1998).
- ⁷S. Reboh, A. A. de Mattos, J. F. Barbot, A. Declémy, M. F. Beaufort, R. M. Papaléo, C. P. Bergmann, and P. F. P. Fichtner, *J. Appl. Phys.* **105**, 093528 (2009).
- ⁸L. Shao, Z. Di, Y. Lin, Q. X. Jia, Y. Q. Wang, M. Nastasi, P. E. Thompson, N. D. Theodore, and P. K. Chu, *Appl. Phys. Lett.* **93**, 041909 (2008).
- ⁹P. F. P. Fichtner, J. R. Kaschny, R. A. Yankov, A. Mücklich, U. Kreißig, and W. Skorupa, *Appl. Phys. Lett.* **70**, 732 (1997).
- ¹⁰N. Hueging, M. Luysberg, H. Trinkaus, K. Tillmann, and K. Urban, *J. Mater. Sci.* **41**, 4454 (2006).
- ¹¹S. Reboh, M. F. Beaufort, J. F. Barbot, J. Grilhé, and P. F. P. Fichtner, *Appl. Phys. Lett.* **93**, 022106 (2008).
- ¹²J. F. Ziegler and J. P. Biersack, SRIM computer code at the URL <http://www.srim.org> (2008).
- ¹³M. Hartmann and H. Trinkaus, *Phys. Rev. Lett.* **88**, 055505 (2002).
- ¹⁴H. Tada, P. C. Paris, and G. C. Irwin, *The Stress Analysis of Cracks Handbook* (ASME, New York, 2000).
- ¹⁵D. Gross and T. Seelig, *Fracture Mechanics with an Introduction to Micromechanics* (Springer, Netherlands, 2006).
- ¹⁶R. Gibala and R. F. Hehmann, *Hydrogen Embrittlement and Stress Corrosion Cracking* (ASM, Metals Park, OH, 1984).